

---

*Research Article: Methods/New Tools | Novel Tools and Methods*

## **Real-time selective markerless tracking of forepaws of head fixed mice using deep neural networks**

<https://doi.org/10.1523/ENEURO.0096-20.2020>

**Cite as:** eNeuro 2020; 10.1523/ENEURO.0096-20.2020

Received: 11 May 2020

Revised: 16 April 2020

Accepted: 7 May 2020

---

*This Early Release article has been peer-reviewed and accepted, but has not been through the composition and copyediting processes. The final version may differ slightly in style or formatting and will contain links to any extended data.*

**Alerts:** Sign up at [www.eneuro.org/alerts](http://www.eneuro.org/alerts) to receive customized email alerts when the fully formatted version of this article is published.

Copyright © 2020 Forys et al.

This is an open-access article distributed under the terms of the Creative Commons Attribution 4.0 International license, which permits unrestricted use, distribution and reproduction in any medium provided that the original work is properly attributed.

1 **1) Manuscript Title:** Real-time selective markerless tracking of forepaws of head fixed mice  
2 using deep neural networks.

3 **2) Abbreviated title:** Real-time tracking of mouse body parts using deep neural networks.  
4

5 **3) Authors:** Brandon J Forys<sup>1,2†</sup>, Dongsheng Xiao<sup>1†</sup>, Pankaj Gupta<sup>1</sup>, Timothy H Murphy<sup>1</sup>

6 <sup>1</sup>Department of Psychiatry, Kinsmen Laboratory of Neurological Research, University of British  
7 Columbia, Vancouver, British Columbia, Canada

8 <sup>2</sup>Department of Psychology, Djavad Mowafaghian Centre for Brain Health, University of British  
9 Columbia, Vancouver, British Columbia, Canada

10 <sup>†</sup>Co-first authors

11

12 **4) Contributions:** B.F. and D.X. designed research, performed research, contributed analytic  
13 tools, analyzed data, and wrote the paper. P.G. contributed analytic tools. T.H.M. designed  
14 research and wrote the paper.

15

16 **5) Correspondence should be addressed to:** Timothy H Murphy

17 Address: 2255 Wesbrook Mall, Detwiller Pavilion, Vancouver, B.C. V6T 1Z3, Canada

18 E-mail: thmurphy@mail.ubc.ca

19

20 **6) Number of figures:** 7

21 **7) Number of tables:** 2

22 **8) Number of multimedia:** 1

23 **9) Number of words in abstract:** 187

24 **10) Number of words in significance statement:** 79

25 **11) Number of words in introduction:** 539

26 **12) Number of words in discussion:** 2395

27

28 **13) Acknowledgements:** We thank Pumin Wang and Cindy Jiang for surgical assistance and  
29 technical assistance. We thank Rene Tandun for assisting in pose estimation model training. We  
30 thank Jamie D Boyd and Hao Hu for technical assistance and Braeden Jury for helpful  
31 discussions and suggestions.

32

33 **14) Conflict of Interest:** Authors report no conflict of interest.

34

35 **15) Funding Sources:** This work was supported by Canadian Institutes of Health Research  
36 (CIHR) Foundation Grant FDN-143209 to T.H.M., THM is supported by the Brain Canada  
37 Neurophotonics Platform and the Canadian Partnership for Stroke Recovery. D.X. was  
38 supported in part by funding provided by Brain Canada, in partnership with Health Canada, for  
39 the Canadian Open Neuroscience Platform initiative. D.X. was supported in part by funding  
40 provided by Brain Canada, in partnership with Health Canada, for the Canadian Open  
41 Neuroscience Platform initiative.

42 **ABSTRACT**

43 Here, we describe a system capable of tracking specific mouse paw movements at high frame  
44 rates (70.17 Hz) with a high level of accuracy ( $M = 0.95$ ,  $SD = 0.01$ ). Short-latency markerless  
45 tracking of specific body parts opens up the possibility of manipulating motor feedback. We  
46 present a software and hardware scheme built on DeepLabCut – a robust movement-tracking  
47 deep neural network framework – that enables real-time estimation of paw and digit movements  
48 of mice. Using this approach, we demonstrate movement-generated feedback by triggering a  
49 USB-CGPIO controlled LED when the movement of one paw, but not the other, selectively  
50 exceeds a pre-set threshold. The time delay between paw movement initiation and LED flash  
51 was  $M = 44.41$  ms,  $SD = 36.39$  ms, a latency sufficient for applying behaviorally-triggered  
52 feedback. We adapt DeepLabCut for real-time tracking as an open-source package we term  
53 DeepCut2RealTime. The package’s ability to rapidly assess animal behavior was demonstrated  
54 by reinforcing specific movements within water-restricted, head-fixed mice. This system could  
55 inform future work on a behaviorally triggered ‘closed loop’ brain-machine interface that could  
56 reinforce behaviors or deliver feedback to brain regions based on pre-specified body movements.

57 **Significance statement**

58 We present a software and hardware scheme modified from DeepLabCut – a robust movement-  
59 tracking deep neural network framework – that enables real-time estimation of paw and digit  
60 movements of mice. Coupled to the body part tracking is the ability to rapidly trigger external  
61 events such as rewards upon the detection of specific behaviors. This system lays the  
62 groundwork for a behaviorally triggered ‘closed loop’ brain-machine interface that could  
63 reinforce behaviors and deliver feedback to brain regions based on pre-specified body  
64 movements.

65 **INTRODUCTION**

66           The accurate quantification and manipulation of behavioral dynamics of animals is  
67 important for understanding the neural basis of motor function (Jin and Duan, 2019; Moreira et  
68 al., 2019). Real-time movement tracking is a challenging computer vision problem that is crucial  
69 for constructing precise movement-triggered feedback systems and brain-machine interfaces  
70 (BMIs) needed for mechanistic studies of animal behavior. Furthermore, real-time movement  
71 tracking and feedback would enable rapid reinforcement of user-defined behaviors of interest.  
72 Significant progress in the development of movement tracking technology enables accurate pose  
73 estimation in humans (Insafutdinov et al., 2016) and animals (Mathis et al., 2018) without the  
74 need to manually label large datasets as inputs for training. In particular, with regards to tracking  
75 animal movement, the approach presented by Mathis et al.'s DeepLabCut toolbox (Mathis et al.,  
76 2018) generalizes well across morphologically diverse animals. Traditional methods of tracking  
77 movement are often based on large databases of stereotyped movement data, such as those used  
78 by Insafutdinov et al. for pose estimation (2016). In contrast, the DeepLabCut approach (Mathis  
79 et al., 2018) enables users to generate models that can be more sensitive to movements of a  
80 variety of animals under laboratory conditions using a smaller dataset. While DeepLabCut is a  
81 robust tool for pose estimation (Mathis et al., 2018), it has primarily been used for post-hoc  
82 analysis of behavior and not in real-time. A customizable framework for real-time tracking of  
83 specific body parts in target subjects would have many applications in psychiatry, rehabilitation  
84 engineering, and other fields where closed-loop feedback is employed. An interesting application  
85 and future work direction would be to investigate cortical regions involved in the coordination  
86 and planning of movements when used in combination with optogenetics (Ayling et al., 2009;

87 Guo et al., 2015; Mathis et al., 2017). In addition to rapid feedback, real-time analysis would  
88 permit behavioral reinforcement by coupling specific movements to reward.

89

90 To use high-resolution video and markerless pose estimation as an input for real-time  
91 feedback, we require a robust system that can process and track individual body parts with low  
92 latency. However, the majority of low-latency real-time tracking systems are based on blob  
93 detection algorithms (Chaumont et al., 2018; Kim et al., 2018), or rely on post hoc classification  
94 of movement (Gabriel et al., 2019) or highly specialized behavioral arenas that collect data  
95 through multiple modalities (Moreira et al., 2019). Such methods, while often less  
96 computationally intensive than pose estimation algorithms, are better suited to whole-body  
97 tracking than body part tracking. The few markerless tracking systems that do exist typically  
98 require extensive, specialized body part detection logic (Mathis and Mathis, 2020; Sehara et al.,  
99 2019), rendering them relatively inflexible across different animals. As such, while previous  
100 approaches to real-time tracking are effective for examining social interactions or holistic body  
101 movements, they are typically unable to selectively discern small-scale movements – such as  
102 whisker, digit, or nose movements. We present adaptations to DeepLabCut (Mathis et al., 2018)  
103 to leverage it for real-time movement tracking and analysis based on the conditional movement  
104 of individual body parts in head-fixed mice with latencies that averaged  $44 \pm 36$  ms (Study 1).  
105 Additionally, we validate our real-time feedback system by using it to train a group of water-  
106 restricted, head-fixed mice to make user-defined forepaw movements (Study 2).

107

108 **Materials and methods**

109 Animal protocols (A13-0336 and A14-0266) were approved by National Use guidelines.  
110 Animals were housed in a vivarium on a 12 h day light cycle (7 AM lights on). For head fixation  
111 hardware surgery (Silasi et al., 2016), animals were anesthetized with isoflurane (2% in pure O<sub>2</sub>)  
112 and body temperature was maintained at 37°C using a feedback-regulated heating pad monitored  
113 by a rectal thermometer while they received a cranial window. Mice received an intramuscular  
114 injection of 40 µl of dexamethasone (2 mg/ml) and a 0.5 ml subcutaneous injection of a saline  
115 solution containing buprenorphine (2 µg/ml), atropine (3 µg/ml), and glucose (20 mM), and were  
116 placed in a stereotaxic frame. After locally anesthetizing the scalp with lidocaine (0.1 ml, 0.2%),  
117 the skin covering the skull was removed and replaced by dental cement (Ayling et al., 2009; Hira  
118 et al., 2009; Silasi et al., 2016). A metal screw was attached to the chamber for future head  
119 fixation during experiments. At the end of the procedure, the animal received a second  
120 subcutaneous injection of saline (0.5 ml) with 20 mM of glucose and recovered in a warmed  
121 cage for 30 min.

122  
123 For the first study, head-fixed mice (male) were stabilized by attaching a skull-mounted  
124 screw to a pole mounted on a base-plate while the body was resting in a tube (Silasi et al., 2016).  
125 We attach an LED to this pole so that it is visible in the video recording of the mouse, enabling  
126 ground-truth validation of the behavioral feedback paradigm by quantifying the resulting light  
127 flash.

128  
129 For a second study investigating our system's ability to automatically reinforce mice for  
130 making specific movements, mice (male, n=8) underwent head-bar surgery and were trained to  
131 learn a movement-related task under a head-fixed condition. Before starting the behavioral

132 training, ad libitum access to water was stopped. Mice were handled daily and received 1 mL of  
133 water per day until they reached ~85% of initial weight (typically 5–7 days after the start of  
134 water restriction). During the handling period, mice were habituated to the experimental setup.  
135 The duration of head fixation was progressively increased at a rate of 5 min/day. Handling and  
136 head restraining were performed by taking care to minimize the discomfort of the animals. For  
137 the task, these mice were head-fixed and positioned as in the first study. In addition to the setup  
138 described in the first study, a waterspout was placed ~3 mm in front of the mouse's mouth, such  
139 that the mouse could only acquire water after making a movement with its paw that was  
140 quantified by real-time tracking.

141

142 **Training movement tracking models.** We use DeepLabCut 2.0.6 (Mathis et al., 2018)  
143 as the basis for our movement tracking framework. A general model of mouse paw movement  
144 was trained based on ResNet-50 by labelling 200 frames selected using k-means clustering (Nath  
145 et al., 2019) in order to sample a variety of movement dynamics from one video of each of the 10  
146 mice recorded ( $N = 10$  videos). These videos were recorded using an Omron Sentech STC-  
147 MCCM401U3V USB3 Vision camera through the StCamSWare software (Omron Sentech Co  
148 Ltd., Kanagawa, Japan) at a resolution of 256x256 px. To generate this model, we labelled the  
149 tips of all eight toes on both forepaws in videos of mice recorded in a similar environment and  
150 lighting conditions as the environment for the final behavioral trials for each mouse. We trained  
151 our model for 35,000 iterations, with a 95% train-test split (Fig. 1). All image processing,  
152 tracking, and LED output was carried out on an ASUS All Series computer running Windows  
153 8.1 with 64 GB of RAM, 3.4 GHz, 64 GB of RAM, and an Nvidia Titan Xp GPU.

154

155           **Real-time tracking.** We stream a video of each mouse ( $N = 10$ ) to the desktop computer  
156 using an Omron Sentech STC-MCCM401U3V USB3 Vision camera (Omron Sentech Co Ltd.,  
157 Kanagawa, Japan) at a resolution of 256x256 px for 130 seconds (Fig. 2A).

158

159           To allow the framerate and DeepLabCut's computations to stabilize, we run the  
160 movement analysis, but do not save the analysis or provide feedback, for the first 10 seconds of  
161 each trial; as such, we record 120 seconds of movement and feedback data for each trial. This  
162 10-second buffer period allows a large number of threads that are necessary for rapid  
163 computations to start. The base version of DeepLabCut is optimized to process existing video  
164 frames within batches at a high speed. When tracking and reinforcing animal behavior in near  
165 real-time, we do not have the luxury of letting several frames pool into a batch before conducting  
166 simultaneous pose estimation and behavioral feedback on all frames in the batch, as this would  
167 delay feedback to the animal that is dependent on the pose estimation. As such, we prioritize  
168 faster processing of smaller batches in order to rapidly deliver feedback to the animal based on a  
169 guaranteed comparison between consecutive frames. The best strategy we were able to find to  
170 accomplish this rapid processing is the simultaneous creation of numerous parallel threads that  
171 take in video input, estimate the animal's pose, and output the feedback signal. For every batch  
172 of two frames from the camera, our system creates four threads (Fig. 2). These threads are shut  
173 down once they are finished; however, for the first 10 seconds, the number of threads created  
174 exceeds the number of threads being destroyed. After the first 10 seconds, threads are created  
175 and destroyed at a relatively stable rate, easing computational load and improving the stability of  
176 the frame-rate. We found that 10 seconds was the minimum buffering time required to achieve a  
177 stable frame rate for the rest of the task.



178 To test the performance of the tracking and feedback at various frame rates, we set the  
179 input frame rate of the camera to 90 Hz for 13 trials, 180 Hz for 13 trials, 200 Hz for 13 trials,  
180 220 Hz for 7 trials, 270 Hz for 14 trials, 300 Hz for 11 trials, 320 Hz for 9 trials, and 360 Hz for  
181 1 trial (Table 1). We varied the camera's framerate from 90 to 360 Hz and assessed the  
182 specificity of tracking. A range of frame rates was tried with some higher frame rates showing  
183 errors, and 200 Hz offered an optimal compromise between tracking efficiency and trigger  
184 latency. Two trials – one recorded at 220 Hz and one recorded at 360 Hz – were excluded  
185 because of program runtime issues leading to mean delays of over 500 ms. One trial recorded at  
186 270 Hz was excluded because the mouse did not move enough to exceed the minimum  
187 movement threshold, resulting in no triggers above criterion for this trial. There were 27 trials in  
188 which the mouse briefly engaged in grooming behavior; while this resulted in behavioral triggers  
189 being sent, it did not affect the tracking accuracy or delay of feedback. The shutter speed of the  
190 camera was set to 1/500 s for all trials. We use the pysentech library  
191 (<https://github.com/derricw/pysentech>) to allow Python to interface with the camera. As each  
192 video frame arrives on the computer, we convert it to an 8-bit unsigned byte format and pass it to  
193 DeepLabCut's pose analysis function in a batch of two consecutive frames, in a separate thread  
194 for each batch (Fig. 2A). This function returns the predicted positions of each toe on the mouse's  
195 left paw. In an additional thread (Fig. 2E), we render these coordinates onto the newly analyzed  
196 frame using opencv2 (<https://opencv.org/>) to enable visual inspection of tracking quality.

197

198 **Real-time feedback.** In order to deliver feedback based on specific paw movements we  
199 define a target paw movement to reinforce. We operationalize this paw movement as a difference  
200 in the average vertical position of the four estimated toe positions on the mouse's left paw from

201 one frame to the next that is greater than a minimum but smaller than a maximum threshold that  
202 we define. These thresholds ensure that small shifts in the mouse's paw, or large errors in  
203 tracking, do not result in erroneous feedback to the animal. We chose to track the mouse's  
204 vertical movement of its left paw because this movement approximates a reaching activity,  
205 which is an example of a movement that could be conditioned using our feedback paradigm.  
206 Based on the frame's resolution and our mouse's paw movements, we set the minimum threshold  
207 as 5 pixels of vertical movement of the mouse's left paw, and the maximum threshold as 100  
208 pixels of vertical movement of this paw (to prevent feedback being delivered if the tracking  
209 erroneously jumps across the screen). To help ensure that the feedback was selective for left paw  
210 movement, no feedback was delivered if the mouse's right paw exceeded 10 pixels of vertical  
211 movement, regardless of left paw movement (Fig. 2D). We set the right paw movement limit  
212 threshold as twice as large as the threshold for the left paw because we found that the initial  
213 group of mice that we assessed were prone to making more spontaneous right-paw movements  
214 than left paw movements. A strict restriction of 5 pixels on both paws (right paw no more than 5  
215 pixels and left paw at least 5 pixels) was associated with an overall decreased number of triggers  
216 as even small, unreinforced right paw movements often occurred at the same time as left-paw  
217 movements. Importantly, the software we provide is flexible, and the criterion can be set to  
218 reflect the movement of any set of tracked points. If the vertical movement of the left paw from  
219 one frame to the next is between 5 and 100 px inclusive, we give visual feedback using a trigger  
220 set by the pyftdi library (<https://github.com/eblot/pyftdi>) to turn on a red LED on the head-fixing  
221 pole for 200 ms over USB via an Adafruit FT232h breakout board (Adafruit Industries, New  
222 York, NY) (Fig. 2G). As a further safeguard against erroneous triggering of feedback, this  
223 feedback is only triggered if DeepLabCut determines that the body part prediction accuracy for

224 that frame (quantified as the output of the TensorFlow sigmoid function) is greater than 0.20.  
225 Lastly, in order to ensure that feedback is not continuously delivered to the mouse in the event of  
226 repeated paw movement above threshold we set a refractory period of 300 ms after each trigger  
227 during which no trigger is delivered regardless of movement dynamics (for three mice across 21  
228 trials).

229

230 In a second study, we validated our method's ability to assess and reinforce a user-  
231 defined behavior in real time. Mice were presented with alternating baseline and training trials ( $n$   
232 = 115 baseline, 115 training) across 5 days. Each of these trials had the same length, structure,  
233 and computational analyses of behavior used in the first study. Mice were cued to training trials  
234 by the illumination of a green LED located ~20 mm to the left and above the mouse's head, for  
235 the duration of the trial. On training trials, the mouse received water for 150 ms from the  
236 waterspout in front of its mouth if it made a criterion forelimb movement (greater than or equal  
237 to 5 pixels of vertical movement of the left paw while simultaneous movement on the right paw  
238 was less than 10 pixels). In this study, the mouse was not rewarded for making exclusively right-  
239 paw movements and making a right-paw movement following a left-paw one increased the  
240 probability of not receiving a reward. The use of the 10-pixel right paw movement limit criterion  
241 increased the ability to reward selective left-paw movements. This water reward was  
242 accompanied by the illumination of a red LED located ~20 mm to the left and above the mouse's  
243 head for 200 ms. In comparison, on baseline trials, the mouse did not receive feedback for  
244 making a criterion forelimb movement, and the green LED did not illuminate for the length of  
245 the trial. However, the red LED continued to flash when the mouse made the criterion  
246 movement. In order to have a consistent ground-truth measure of the mouse making the

247 reinforced movement trials were recorded using the same methodology as outlined in the first  
248 study. All trials in the second study were recorded at 200 Hz, as this was the framerate that  
249 offered the best combination of a high framerate and low feedback latency in the first study  
250 (Table 1).

251

252 **Code Accessibility.** We provide a Python script to enable real-time tracking within the existing  
253 DeepLabCut 2 workflow, and a modified set of pyftdi classes to allow interfacing between  
254 Python and the GPIO board. This code is freely available online at  
255 <https://github.com/bf777/DeepCut2RealTime>. We also provide a MATLAB script to enable  
256 automatic analysis of behavior videos collected in real-time. This code is freely available online  
257 at <https://github.com/DongshengXiao/RealTimeTracking>. We provide copies of this acquisition  
258 and analysis software online as extended data.

259

## 260 **Results**

261 **Behavioral model.** The behavioral model that we trained to predict the mouse's  
262 movements in DeepLabCut had a root mean squared error (RMSE) of prediction of 2.17 pixels  
263 for the training data and 2.37 pixels for the test data when using a standard scene that averaged  
264 44 x 44 mm (visualized in Fig. 1A).

265

266 **Real-time tracking.** We recorded a total of 81 trials across 9 mice, with each trial being  
267 130 s in length. A total of 78 trials across these 9 mice were analyzed (see Methods for exclusion  
268 explanation). We quantified the behavioral tracking quality of each trial by calculating the  
269 average frame rate over 120 s (after the conclusion of the 10 s buffer period), and the average

270 accuracy of each prediction in each frame being correct as measured by the TensorFlow sigmoid  
271 function as implemented in DeepLabCut. The mean tracking accuracy across all trials was 0.95,  
272  $SD = 0.01$ . Input frame rates were much higher than the output frame rates, suggesting that  
273 some frames were dropped. For example, an input frame rate of 200 Hz would yield an output  
274 rate of frame rate of 70 Hz. While the dropping of frames is concerning, we do record the frame  
275 times for reconstruction of time courses. Lower frame rates of 90 Hz dropped fewer frames,  
276 leading to an output framerate of ~45 Hz (Table 1).

277

278       **Real-time feedback.** To evaluate the delay between frame acquisition and the LED flash  
279 that signalled a movement that reached criterion, we record the time at which the frame was sent  
280 from the camera, the time at which the feedback criterion was met, and the time at which the  
281 LED turned on based on the collected video which contains the behavioral video of the mouse.  
282 Plotting the movement of the left and right paws for trials where trigger conditions were met  
283 indicated – as expected – a preference for left paw over right paw movement (Fig. 3).  
284 Importantly, the LED trigger was delivered within ~40 ms of the left paw crossing the threshold  
285 which was estimated to be a 0.85 mm movement. We quantified the feedback latency as the  
286 average delay between frame acquisition and feedback delivery on trials. This delay was  
287 measured by timestamps from Python where movement of the left paw exceeded the minimum  
288 threshold and was below the maximum threshold while – simultaneously – movement in the  
289 right paw was below the maximum threshold for that paw. Across all trials, the delay between  
290 movement initiation and LED illumination across trials ( $N = 9$  mice, 78 trials) was  $M = 44.41$   
291 ms,  $SD = 36.39$  ms (Fig. 4). Summary statistics broken down by input framerate are outlined in  
292 Table 1. We depict typical behavioral reinforcement of the mouse in Video 1.

293

294           In order to provide a second ground-truth measure of feedback latency and verify these  
295 delay values, we recorded a second set of trials ( $N = 5$ ) with a 200 Hz frame rate in which the  
296 LED illumination was readily visible within the video frame, offering a visual indicator of the  
297 feedback onset. We used MATLAB (2014b, The MathWorks, Inc., Natick, MA, United States)  
298 to define a region of interest surrounding the LED in each recording and quantified each LED  
299 illumination as a change in pixel value greater than three standard deviations from the mean  
300 background. As an increased number of frames were dropped within the first 800 frames of each  
301 trial (~4 s; Fig. 3) we quantified the LED illumination time after the 800<sup>th</sup> frame. We then  
302 quantify ground-truth latency as the time between the start of the frame on which a significant  
303 movement was detected, and the point at which the LED illumination crosses the criterion value  
304 discussed above. The mean ground-truth latency calculated through this method was 35.90 ms;  
305 the mean latency calculated through the timestamps in the code was 32.40 ms. We found no  
306 significant difference between the ground-truth latency and the timestamp latency ( $t(4) = 0.76$ ,  $p$   
307  $= 0.54$ ). The average waveform of the LED flash for an example trial is given in figure 4A; the  
308 overall waveform for the LED flash is plotted alongside behavioral triggers in figure 4B.

309

310           For our second study – in which we reinforced mice for making movements that  
311 exceeded the criterion discussed for the first study – we analyzed five days of training from  
312 seven mice. Although we had eight mice total, we excluded one mouse from our analyses as that  
313 mouse did not run on all five days. We analyzed a total of 102 baseline and 102 training trials  
314 (21 trials of each type per day except on the second day of training, where there were 18 trials of  
315 each type). For the summary data for the second study (Table 2), we only excluded one training

316 trial of one mouse who did not make any movements above criterion. Comparing the average  
317 number of movement triggers made for baseline and training trials allowed us to quantify the  
318 overall success of our automated reinforcement paradigm at motivating the forelimb movement  
319 behavior of the mouse (Fig. 5A). Based on paired-sample t-tests with Bonferroni correction for  
320 multiple comparisons between each day's training trials and training trials on the first day, the  
321 average number of above-threshold movements was significantly greater in training trials on the  
322 third, fourth, and last days of training compared to training trials on the first day of training (Fig.  
323 5A). There were no significant differences in above-threshold movements between each day's  
324 baseline trials and baseline trials on the first day. Based on paired-sample t-tests with Bonferroni  
325 correction for multiple comparisons between each day's training trials and baseline trials, there  
326 was a significant difference in above-threshold movements between training and baseline trials  
327 on the third day. In order to further validate the selectivity of our system for left-paw movement,  
328 we evaluated the number of right-paw movements greater than 10 pixels (the maximum criterion  
329 for right-paw movement in order to receive a reward) for each frame immediately following a  
330 successful left-paw trigger (Fig. 5B). Based on paired-sample t-tests Bonferroni correction for  
331 multiple comparisons, we found no significant differences between days or between baseline or  
332 training trials in the number of right-paw movements greater than 10 pixels immediately  
333 following above-threshold left-paw movements. Across all trials, the average number of these  
334 right-paw movements  $> 10$  pixels was lower than the average number of immediately preceding  
335 left-paw movements  $\geq 5$  pixels.

336

337         Animals were reinforced based on the average movement of all four digits of their paws.

338 However, we also investigated whether the movement of each individual digit aligned with this

339 average movement. As a follow-up analysis, we evaluated the number of left-paw digit  
340 movements  $\geq 5$  pixels (Fig. 6A) as well as the number of right-paw digit movements  $> 10$   
341 pixels (the maximum criterion for right-paw movement in order to receive a reward) for each  
342 digit individually (Fig. 6B). Overall, we found a similar pattern of vertical movements across  
343 each digit to the mean movement of each paw (Fig. 5), suggesting that individual digits could  
344 potentially also be useful as targets for behavioral reinforcement. Additionally, we conducted  
345 ANOVAs for each digit on training and baseline trials and found no significant difference  
346 between digits on the number of movements above criterion on baseline or training trials on each  
347 day, on either forepaw.

348

349       As an alternative analysis that does not rely on frequentist statistics, we used the Data  
350 Analysis with Bootstrap Estimation in R (dabestr) package (Ho et al., 2019) recommended by  
351 Calin-Jageman and Cumming (2019) to conduct a set of estimation statistical analyses. Bootstrap  
352 resampling is a robust statistical method that allows for more precise conclusions about patterns  
353 of data (Calin-Jageman and Cumming, 2019). Our analyses present the bootstrapped 95%  
354 confidence interval surrounding the mean difference between the number of above-threshold  
355 movements on baseline and training trials on each day (Fig. 7A); the mean difference between  
356 the number of number of above-threshold movements during training trials on each day to  
357 training trials on the first day (Fig. 7B); and the corresponding mean difference comparisons for  
358 baseline trials on each day (Fig. 7C). The 95% confidence interval for the mean difference  
359 between the number of above-threshold movements on baseline and training trials on each day  
360 does not cross 0 (Fig. 7A). As such, we can say that each animal makes more above-threshold  
361 forepaw movements during training trials as compared to baseline trials. Furthermore, the 95%



362 confidence intervals for the mean difference between the number of number of above-threshold  
363 movements during training trials on each day to training trials on the first day do not cross 0 for  
364 training trials for days 3, 4, and 5 (Fig. 7B). Therefore, we can also say that the animals overall  
365 make more above-threshold forepaw movements after two days of training (Fig. 7B) while not  
366 making more of these movements on progressive baseline trials (Fig. 7C).

367

## 368 **DISCUSSION**

369 We demonstrate a robust real-time tracking and feedback paradigm implemented in  
370 Python that can deliver feedback based on individual body part movement with a short delay  
371 between movement initiation and LED illumination. Generally, we observed that this delay  
372 resulted in the LED being illuminated while the movement that triggered the LED was still in  
373 progress (Fig 3B, C). This relatively fast feedback based on specific body movements in near-  
374 real time suggests that our interface could be adapted to provide any type of feedback that is  
375 driven by a GPIO signal, including delivery of a water reward or an optogenetic pulse.  
376 Additionally, our feedback system, given a robust behavioral model, enables sensitivity to the  
377 movements of a single body part, as demonstrated by the system delivering feedback when the  
378 left paw moves independently of the right paw. Lastly, we demonstrate our system's ability to  
379 condition and reinforce user-defined behaviors using a water restriction paradigm.

380

### 381 **Real-time feedback system**

382 Our conclusion is that input framerates of 200 Hz are optimal for analysis and feedback  
383 generation. Increased work on code stability may enable the use of higher input framerates,  
384 allowing for the measurement of more rapid behaviors. The difference between the input

385 framerate – the framerate set on the camera – and the output framerate – the rate at which frames  
386 were processed by our system – likely differs because of the added computational load that  
387 DeepLabCut places on the acquisition and analysis system. The most significant factors affecting  
388 this framerate appeared to be 1.) the method by which we saved the labelled frames (saving  
389 frames asynchronously, as opposed to in the same thread as the threshold computations, provided  
390 an improvement of 20-50 Hz at all framerates tested) and 2.) the capabilities of the USB port to  
391 which the camera was connected (connecting the camera to a faster USB 3 port provided an  
392 improvement of 20-50 Hz at all framerates tested). We were also able to minimize this  
393 computational load by running DeepLabCut’s pose estimation framework while not saving the  
394 outputs for a period of 10 seconds at the beginning of each trial (Fig. 3D). We believe that  
395 providing this buffer period has the effect of allowing Python libraries and the complex neural  
396 network architecture of DeepLabCut to load.

397

398         A number of factors potentially affected the quality of the tracking. Firstly, deviations  
399 from the lighting conditions of the videos on which we trained our models occasionally resulted  
400 in tracking of spurious body parts (such as the ear) or arbitrary points. In particular, regions of  
401 the video with high contrast relative to the intended body parts occasionally became the focus for  
402 tracking, especially when lighting conditions were incorrect. This may be a function of how the  
403 scoremap calculations that are involved in pose estimation are carried out within DeepLabCut  
404 (Mathis et al., 2018). Some lighting changes between the training data and the streamed video  
405 were inevitable; we attempted to mitigate these changes by keeping the location of the mouse  
406 and the lighting in the room where the experiments took place the same as in the training videos.  
407 However, by training our behavioral model for over 30,000 iterations across a video dataset that

408 encompassed a wide variety of behaviors, our model became very accurate in distinguishing one  
409 paw from the other without the need for additional post-processing. In fact, a high level of  
410 accuracy was generally maintained even during grooming behaviors, when the paws' forms were  
411 obscured. This suggests that variations in camera setup and lighting conditions can be  
412 compensated for with a well-labelled and trained behavioral model. Secondly, hardware  
413 limitations may also have contributed to increases in the delay. Although our camera was  
414 connected to a USB 3.0 port, we carried out a small number of trials ( $N = 4$ ) with a faster USB  
415 3.0 port on the computer in order to compare performance with each port on the computer.  
416 Although trials in which the camera was connected to this faster port produced a higher output  
417 frame rate for each level of the input frame rate, this solution resulted in a less stable frame rate,  
418 leading to much higher delays at frame rates beyond 180 Hz. Thirdly, although the pyftdi library  
419 provides a low-level interface between a computer and an LED, the breakout board is connected  
420 via USB 2.0, which presents a hardware bottleneck compared to the USB 3.0 technology used  
421 for our camera. However, the delay between the movement trigger and the LED activation  
422 (measured as the difference in time between the computer timestamp recorded when the left paw  
423 movement criterion was reached, and the timestamp recorded when the signal was sent to turn on  
424 the LED) was very small ( $M = 0.31$  ms,  $SD = 0.13$  ms) and therefore effectively inconsequential  
425 to feedback delivery. Additionally, the mice engaged in grooming behaviors during a number of  
426 trials (as discussed earlier). However, while this presented a challenge to our model's tracking  
427 accuracy – as grooming behaviors were not greatly represented in the training dataset – both the  
428 tracking accuracy and the behavioral feedback remained robust even during these periods of  
429 grooming.  
430

431 We should caution that the method by which accuracy is quantified – TensorFlow’s  
432 sigmoid function, which reflects a comparison between the video stream of the mouse and the  
433 input data provided to the DeepLabCut movement tracking model – is not a ground truth  
434 measure of accuracy. However, this method of quantifying the tracking accuracy has been  
435 validated against ground-truth human ratings by the developers of DeepLabCut (Mathis et al.,  
436 2018). Further progress in increasing the operational speed of DeepLabCut can likely be made  
437 by streamlining the lower-level analytical operations of DeepLabCut and the threading strategy  
438 used. Because the unstable frame throughput rate in the first ten seconds of each trial tended to  
439 lead to large delays between frame acquisition and LED illumination early in the recording  
440 session, we note that a ten-second buffer period (Fig. 3) – during which DeepLabCut carried out  
441 pose estimation while no data was saved – was generally necessary to allow the frame  
442 throughput rate of our system to stabilize. Additionally, at high input frame rates (generally >200  
443 Hz), at the time when the system began to save the data (after the ten second buffer), a number of  
444 frames would be dropped during a period of approximately one second after data saving began.  
445 This period of time is the transition period from data not being recorded to initiation of data  
446 recording, which likely causes a spike in computational load that stabilizes within a second. We  
447 attempted to minimize the number of dropped frames in this period by adjusting the wait period  
448 after the end of the 10-second buffering period and before the initiation of data recording. A 100  
449 ms wait period minimized the number of frames dropped during the transition period. We  
450 quantified the number of dropped frames by counting the number of data placeholders in our  
451 data structure that lacked data; placeholder rows that lacked data were presumed to be dropped  
452 frames. If a movement occurred during this period of frame drops, the delay was generally well  
453 above average. However, we found that this frame drop generally has little bearing on the delay

454 for the rest of the recording session. Additionally, as we have timestamp data for each frame  
455 start, behavioral trigger, and LED/water release time, we do not rely on the number of frames in  
456 a given trial for analysis.

457

458         The most critical consequence of dropped frames would be inappropriate timing for the  
459 delivery of feedback to the animal. To address this issue, our system makes a decision about  
460 whether or not to provide feedback based on two frames of data that are consecutively received  
461 from the camera are analyzed together. If a frame is dropped from the camera, these two frames  
462 may not be chronologically consecutive. However, our stable framerate suggests that frames are  
463 dropped at a consistent rate (Fig. 3E). Specifically, the standard deviation of the time difference  
464 between frames was very low (SD = 4.16 ms) across all N = 806,153 batches of two frames  
465 collected on training and baseline trials outside of the buffer period. According to the Nyquist-  
466 Shannon sampling theorem (Shannon, 1949), in order to capture all of the animal's behaviors,  
467 our frame rate would need to be at least double the frequency of the fastest movement that we are  
468 sampling. Given that our average frame rate for our second study was 65.59 Hz, we would be  
469 able to sample movements at frequencies of up to 32.80 Hz. In a study of mouse locomotion and  
470 whisking movement, the maximum stride frequency attained by the mouse was 3-4 Hz, and the  
471 peak whisking frequency was 15-20 Hz (Sofroniew et al., 2014). These movements are among  
472 the fastest that a mouse can perform – faster than the forepaw movements that we measured in  
473 our study – and yet they would theoretically be detectable by our system at the output frame rate  
474 of ~65 Hz given that they are less than 32.80 Hz. As such, in spite of the frame loss, our  
475 paradigm should be able to capture a wide variety of desired forepaw movements.

476 Further optimizations to the code would require deeper investigation into the most  
477 computationally intensive aspects of DeepLabCut; an especially important area to focus on  
478 would be parallelization of pose estimation operations in DeepLabCut. The occasional  
479 instabilities in our program's frame rate, which necessitated the addition of the buffer period,  
480 may suggest that DeepLabCut prioritizes fast processing of frames over processing these frames  
481 at a stable rate, especially in the first few seconds of the code's operation. These instabilities may  
482 also arise from the creation of a large number of computational threads with no corresponding  
483 destruction of finished threads at the start of the task.

484

485 We have demonstrated the applicability of our system to tracking forepaw movements in  
486 head-fixed mice. However, our software paradigm could be adapted to track and reinforce a  
487 variety of different behaviors in near real-time (e.g. reaching movements, running on a  
488 transparent belt, reaching for pellets or levers). This would entail training a model to track these  
489 behaviors using DeepLabCut's user-friendly interface, then making minor modifications to  
490 conditional statements in our code to adjust the threshold for movement to be reinforced. In its  
491 current state, our system can drive any output that can be triggered by a GPIO logic signal, be it  
492 an LED flash, water pump activation, food pellet release, or stimulating electrode. While we  
493 have focused only on head-fixed behaviors, the video-based nature of our system means that the  
494 animal needs not be head-fixed for accurate movement tracking and reinforcement to occur. The  
495 only requirement is that the model tracking the animal's behavior be well-labeled and trained so  
496 as to accurately capture a variety of movement dynamics. One challenge that must be considered  
497 in adapting the approach to a freely moving animal would be ensuring that the target body parts  
498 can be reliably tracked and are not occluded as the animal transitions to various view angles.

499

500           Our motor movement tracking and feedback paradigm could enable new forms of non-  
501 invasive closed-loop feedback work that uses motor movements in place of (or augmenting)  
502 neural recordings in order to train animals on a task. Further directions for this research may  
503 combine movement tracking with two-photon microscopy to investigate whether DeepLabCut  
504 can be used to condition motor behaviors in mice through closed-loop feedback in near-real time,  
505 with the potential goal of understanding and localizing motor memory (Fu et al., 2012; Gilad et  
506 al., 2018). Additionally, passing our pose estimation through a pre-defined behavioral state space  
507 (Berman et al., 2014) may enable us to evaluate and provide feedback based on more complex  
508 behaviors, opening the door to real-time reinforcement of sophisticated motor activities. We have  
509 released the code for implementing our movement tracking and feedback system as a Python  
510 script that integrates with DeepLabCut version 2 or later. With minor modifications to the logic  
511 by which the feedback is triggered in the code, our system could be adapted to track virtually any  
512 user-defined body part or animal that is defined in a DeepLabCut model. Future developments of  
513 this system would benefit from the inclusion of a more nuanced behavioral classifier that is  
514 trained to identify and trigger feedback based on complex behavioral dynamics and movement  
515 trajectories. Such a classifier could open the door to the rapid training of even complex behaviors  
516 in animals.

517

#### 518 **Validation through behavioral task**

519           In order to demonstrate our real-time feedback system's utility in a real-world context,  
520 we used our system to automatically reinforce water-restricted mice for making forelimb  
521 movements. Mice made significantly more left-paw movements during training trials on later

522 training days than on the first day (Fig. 5A, Fig. 7B) while the number of left-paw movements  
523 remained stable across all baseline trials (Fig. 5A, Fig. 7C). These movements were generally not  
524 accompanied by large right-paw movements (Fig. 5B), demonstrating the selectivity of our  
525 system for reinforcing a specific paw's movement. Furthermore, these movements were  
526 deployed consistently across the whole paw (Fig. 6). Additionally, all mice made more  
527 movements satisfying the criterion on training trials (where they were reinforced) than on  
528 baseline trials (Fig. 7A). Conceivably, it may be easier to train the mouse to make a highly  
529 stereotyped behavior as opposed to merely giving the animal a specific criterion for the extent of  
530 their movement. The fact that our system was nevertheless able to reinforce a wide range of  
531 movements allows for greater training flexibility than a conventional behavioral reinforcement  
532 paradigm such as a lever press in an operant chamber. With minor modifications to the Python  
533 script driving the behavioral feedback, we could set up our system to reinforce a wide variety of  
534 user-defined behaviors in many different animals. For example, our system could be used to  
535 efficiently train a rodent in a stereotyped motor behavior to promote recovery of motor function  
536 post-stroke.

537

### 538 **Conclusion**

539 This project could form the basis for future work on closed-loop behavioral  
540 reinforcement systems that include brain stimulation (Paz et al., 2013; Prsa et al., 2017) and  
541 could be used to explore the basis of various movement-related and somatosensory activities in  
542 the brain (Stubblefield et al., 2013). Such exploratory research could contribute to more  
543 advanced and effective bio-feedback that leverages both neural and non-neural movement data,  
544 adding greater diversity to the types of information signals. With additional reductions to our



545 system's latency, this work could inform brain-machine interfaces, enabling direct reinforcement  
546 of animal behavior based on movement dynamics.  
547

548 **Table 1.** A data table for all trials that were included in the analysis for the first study (legend  
 549 applies to Table 2 as well). “Input framerate” refers to the streaming framerate set in the software  
 550 for our camera; it represents the framerate of the camera without any additional analyses. “Mean  
 551 output framerate” refers to the mean number of frames per second processed by our system  
 552 across all recordings at each input framerate. “SD output framerate” refers to the standard  
 553 deviation in the number of frames per second processed by our system across all recordings at  
 554 each input framerate. “Mean delay” refers to the mean amount of time, in milliseconds, between  
 555 the system receiving a frame that contains a left paw movement exceeding 5 pixels of vertical  
 556 movement, and the system sending a signal to the breakout board to trigger the LED to provide  
 557 feedback for that movement. “SD delay” refers to the standard deviation, in milliseconds, of the  
 558 delay discussed above. “Mean accuracy” refers to the mean output of the sigmoid function by  
 559 TensorFlow for all body parts for all trials at each framerate. “SD accuracy” refers to the  
 560 standard deviation of the output of the aforementioned sigmoid function. “n” refers to the  
 561 number of trials recorded at each frame rate.

562 **Table 1. A data table for all trials run in the first study.**

<i>Input framerate (Hz)</i>	<i>Mean output framerate (Hz)</i>	<i>SD output framerate (Hz)</i>	<i>Mean delay (ms)</i>	<i>SD delay (ms)</i>	<i>Mean accuracy</i>	<i>SD accuracy</i>	<i>n</i>
90	46.95	1.53	34.34	5.94	0.97	0.01	13
180	68.13	5.10	39.85	42.97	0.94	0.02	13
200	70.17	7.07	32.56	10.70	0.95	0.00	13
220	69.31	0.33	33.82	15.10	0.95	0.03	6
270	80.83	18.27	55.93	55.69	0.94	0.01	13
300	91.45	5.27	60.62	77.71	0.94	0.01	11
320	109.76	49.24	53.28	43.80	0.93	0.04	9

563

564 **Table 2. A data table for all trials run in the second study.**

<i>Day</i>	<i>Input framerate (Hz)</i>	<i>Mean output framerate (Hz)</i>	<i>SD output framerate (Hz)</i>	<i>Mean delay (ms)</i>	<i>SD delay (ms)</i>	<i>Mean accuracy</i>	<i>SD accuracy</i>	<i>n</i>
1	200	65.00	0.53	37.00	10.30	0.99	0.00	21
2	200	66.70	18.26	39.50	10.81	0.94	0.01	20
3	200	66.05	0.65	29.69	7.01	0.90	0.04	24
4	200	65.89	0.57	31.03	7.50	0.95	0.02	24
5	200	65.76	0.54	30.96	8.34	0.95	0.03	21

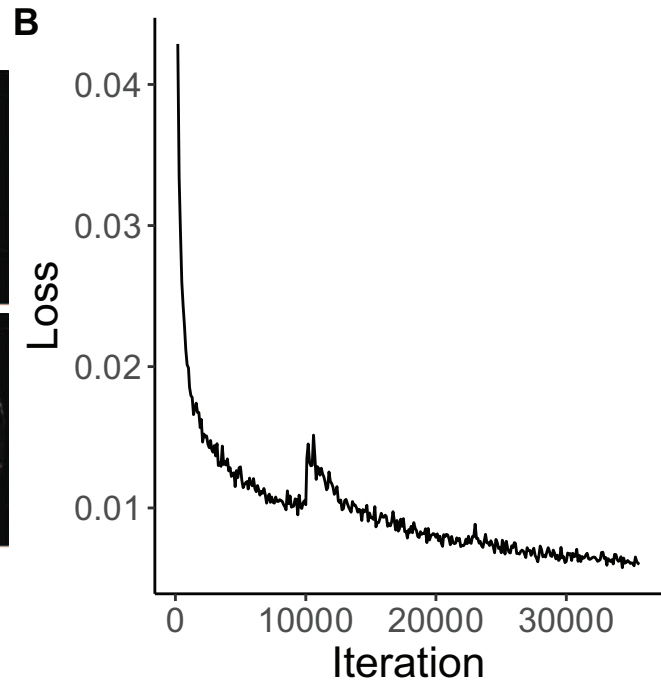
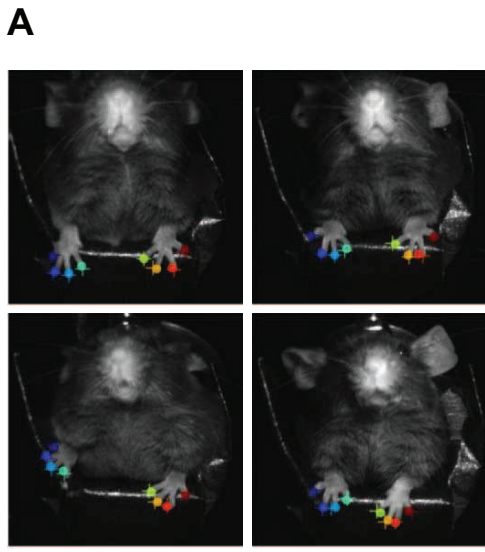
565

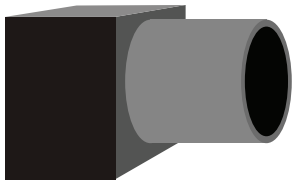
566 **REFERENCES:**

- 567 Ayling OGS, Harrison TC, Boyd JD, Goroshkov A, Murphy TH (2009) Automated light-based  
568 mapping of motor cortex by photoactivation of channelrhodopsin-2 transgenic mice. *Nat*  
569 *Methods* 6:219–224.
- 570 Berman GJ, Choi DM, Bialek W, Shaevitz JW (2014) Mapping the stereotyped behavior of  
571 freely moving fruit flies. *J R Soc Interface* 11.
- 572 Calin-Jageman RJ, Cumming G (2019) Estimation for Better Inference in Neuroscience. *eneuro*  
573 6:ENEURO.0205-19.2019.
- 574 Chaumont F de, Ey E, Torquet N, Lagache T, Dallongeville S, Imbert A, Legou T, Sourd A-M  
575 Le, Faure P, Bourgeron T, Olivo-Marin J-C (2018) Live Mouse Tracker: real-time  
576 behavioral analysis of groups of mice. *bioRxiv* 345132.
- 577 Fu M, Yu X, Lu J, Zuo Y (2012) Repetitive motor learning induces coordinated formation of  
578 clustered dendritic spines in vivo. *Nature* 483:92–96.
- 579 Gabriel PG, Chen K, Alasfour A, Pailla T, Doyle W, Devinsky O, Friedman D, Dugan P,  
580 Melloni L, Thesen T, Gonda D, Sattar S, Wang S, Gilja V (2019) Neural correlates of  
581 unstructured motor behaviors. *J Neural Eng.*
- 582 Gilad A, Gallero-Salas Y, Groos D, Helmchen F (2018) Behavioral Strategy Determines Frontal  
583 or Posterior Location of Short-Term Memory in Neocortex. *Neuron* 99:814-828.e7.
- 584 Guo JZ, Graves AR, Guo WW, Zheng J, Lee A, Rodríguez-González J, Li N, Macklin JJ,  
585 Phillips JW, Mensh BD, Branson K, Hantman AW (2015) Cortex commands the  
586 performance of skilled movement. *Elife* 4:1–18.
- 587 Hira R, Honkura N, Noguchi J, Maruyama Y, Augustine GJ, Kasai H, Matsuzaki M (2009)  
588 Transcranial optogenetic stimulation for functional mapping of the motor cortex. *J Neurosci*  
589 *Methods* 179:258–263.
- 590 Ho J, Tumkaya T, Aryal S, Choi H, Claridge-Chang A (2019) Moving beyond P values: data  
591 analysis with estimation graphics. *Nat Methods* 16:565–566.

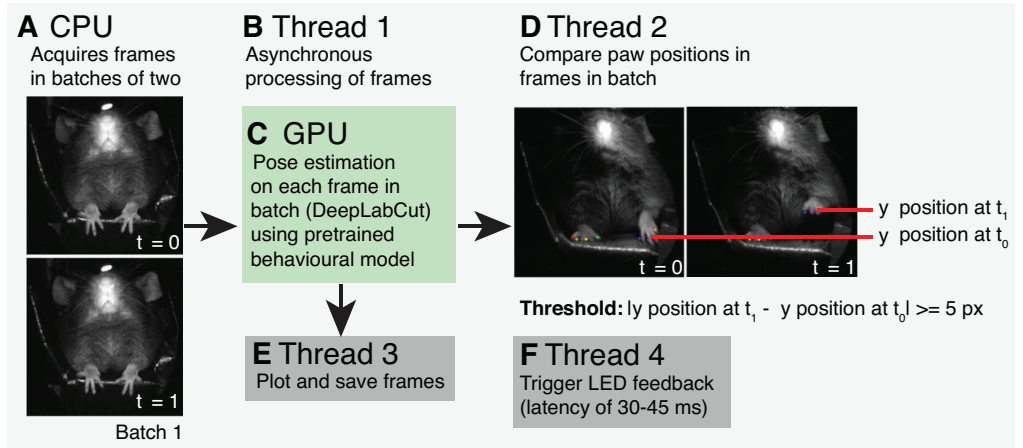
- 592 Insafutdinov E, Pishchulin L, Andres B, Andriluka M, Schiele B (2016) Deepcut: A deeper,  
593 stronger, and faster multi-person pose estimation model. Lect Notes Comput Sci (including  
594 Subser Lect Notes Artif Intell Lect Notes Bioinformatics) 9910 LNCS:34–50.
- 595 Jin T, Duan F (2019) Rat Behavior Observation System Based on Transfer Learning. IEEE  
596 Access 7:62152–62162.
- 597 Kim C, Ruberto T, Phamduy P, Porfiri M (2018) Closed-loop control of zebrafish behaviour in  
598 three dimensions using a robotic stimulus. Sci Rep 8:1–15.
- 599 Mathis A, Mamidanna P, Cury KM, Abe T, Murthy VN, Mathis MW, Bethge M (2018)  
600 DeepLabCut: markerless pose estimation of user-defined body parts with deep learning. Nat  
601 Neurosci 1.
- 602 Mathis MW, Mathis A (2020) Deep learning tools for the measurement of animal behavior in  
603 neuroscience. Curr Opin Neurobiol 60:1–11.
- 604 Mathis MW, Mathis A, Uchida N (2017) Somatosensory Cortex Plays an Essential Role in  
605 Forelimb Motor Adaptation in Mice. Neuron 93:1493-1503.e6.
- 606 Moreira JM, Itskov PM, Goldschmidt D, Baltazar C, Steck K, Tastekin I, Walker SJ, Ribeiro C  
607 (2019) optoPAD, a closed-loop optogenetics system to study the circuit basis of feeding  
608 behaviors. Elife 8:1–19.
- 609 Nath T, Mathis A, Chen AC, Patel A, Bethge M, Mathis MW (2019) Using DeepLabCut for 3D  
610 markerless pose estimation across species and behaviors. Nat Protoc 14:2152–2176.
- 611 Paz JT, Davidson TJ, Frechette ES, Delord B, Parada I, Peng K, Deisseroth K, Huguenard JR  
612 (2013) Closed-loop optogenetic control of thalamus as a tool for interrupting seizures after  
613 cortical injury. Nat Neurosci 16:64–70.
- 614 Prsa M, Galiñanes GL, Huber D (2017) Rapid Integration of Artificial Sensory Feedback during  
615 Operant Conditioning of Motor Cortex Neurons. Neuron 93:929-939.e6.
- 616 Sehara K, Bahr V, Mitchinson B, Pearson MJ, Larkum ME, Sachdev RNS (2019) Fast, Flexible  
617 Closed-Loop Feedback: Tracking Movement in “Real-Millisecond-Time.” *eneuro*  
618 6:ENEURO.0147-19.2019.




- 619 Shannon CE (1949) Communication in the Presence of Noise. Proc IRE 37:10–21.
- 620 Silasi G, Xiao D, Vanni MP, Chen ACN, Murphy TH (2016) Intact skull chronic windows for  
621 mesoscopic wide-field imaging in awake mice. J Neurosci Methods 267:141–149.
- 622 Sofroniew NJ, Cohen JD, Lee AK, Svoboda K (2014) Natural whisker-guided behavior by head-  
623 fixed mice in tactile virtual reality. J Neurosci 34:9537–9550.
- 624 Stubblefield EA, Costabile JD, Felsen G (2013) Optogenetic investigation of the role of the  
625 superior colliculus in orienting movements. Behav Brain Res 255:55–63.
- 626





Camera for real-time streaming of mouse behaviour



-  **Red LED**  
(flash on trigger)
-  **Green LED**  
(cue to training trial)
-  **Waterspout**  
(reward delivery)

**G** Red LED above mouse's head triggers based on paw movement exceeding threshold on baseline and training trials  
 Mouse receives water reward on training trials

